

Supplementary Materials for “A Ready To Use Web-Application Providing a Personalized Biopsy Schedule for Men With Low-Risk PCa Under Active Surveillance”

Anirudh Tomer, MSc^{a,*}, Daan Nieboer, MSc^b, Monique J. Roobol, PhD^c,
Anders Bjartell, MD, PhD^d, Ewout W. Steyerberg, PhD^{b,e}, Dimitris
Rizopoulos, PhD^a, Movember Foundations Global Action Plan Prostate
Cancer Active Surveillance (GAP3) consortium^f

^a*Department of Biostatistics, Erasmus University Medical Center, Rotterdam, the
Netherlands*

^b*Department of Public Health, Erasmus University Medical Center, Rotterdam, the
Netherlands*

^c*Department of Urology, Erasmus University Medical Center, Rotterdam, the Netherlands*

^d*Department of Urology, Skåne University Hospital, Malmö, Sweden*

^e*Department of Biomedical Data Sciences, Leiden University Medical Center, Leiden, the
Netherlands*

^f*The Movember Foundations Global Action Plan Prostate Cancer Active Surveillance
(GAP3) consortium members presented in Appendix F*

1 Appendix A. A Joint Model for the Longitudinal PSA, and Time 2 to Gleason Upgrading

3 Let T_i^* denote the true time of upgrading (increase in biopsy Gleason
4 grade group from 1 to 2 or higher) for the i -th patient included in PRIAS.
5 Since biopsies are conducted periodically, T_i^* is observed with interval cen-
6 soring $l_i < T_i^* \leq r_i$. When upgrading is observed for the patient at his latest

*Corresponding author (Anirudh Tomer): Erasmus MC, kamer flex Na-2823, PO Box
2040, 3000 CA Rotterdam, the Netherlands. Tel: +31 10 70 43393

Email addresses: a.tomer@erasmusmc.nl (Anirudh Tomer, MSc),
d.nieboer@erasmusmc.nl (Daan Nieboer, MSc), m.roobol@erasmusmc.nl (Monique J.
Roobol, PhD), anders.bjartell@med.lu.se (Anders Bjartell, MD, PhD),
e.w.steyerberg@lumc.nl (Ewout W. Steyerberg, PhD), d.rizopoulos@erasmusmc.nl
(Dimitris Rizopoulos, PhD)

7 biopsy time r_i , then l_i denotes the time of the second latest biopsy. Oth-
 8 erwise, l_i denotes the time of the latest biopsy and $r_i = \infty$. Let \mathbf{y}_i denote
 9 his observed PSA longitudinal measurements. The observed data of all n
 10 patients is denoted by $\mathcal{A}_n = \{l_i, r_i, \mathbf{y}_i; i = 1, \dots, n\}$.

In our joint model, the patient-specific PSA measurements over time are modeled using a linear mixed effects sub-model. It is given by (see Panel A, Figure 1):

$$\begin{aligned} \log_2 \{y_i(t) + 1\} &= m_i(t) + \varepsilon_i(t), \\ m_i(t) &= \beta_0 + b_{0i} + \sum_{k=1}^4 (\beta_k + b_{ki}) B_k\left(\frac{t-2}{2}, \frac{\mathcal{K}-2}{2}\right) + \beta_5 \text{age}_i, \end{aligned} \quad (1)$$

11 where, $m_i(t)$ denotes the measurement error free value of $\log_2(\text{PSA}+1)$ trans-
 12 formed [2, 3] measurements at time t . We model it non-linearly over time us-
 13 ing B-splines [4]. To this end, our B-spline basis function $B_k\{(t-2)/2, (\mathcal{K}-2)/2\}$
 14 has three internal knots at $\mathcal{K} = \{0.5, 1.3, 3\}$ years, which are the three quar-
 15 tiles of the observed follow-up times. The boundary knots of the spline are
 16 at 0 and 6.3 years (95-th percentile of the observed follow-up times). We
 17 mean centered (mean 2 years) and standardized (standard deviation 2 years)
 18 the follow-up time t and the knots of the B-spline \mathcal{K} during parameter esti-
 19 mation for better convergence. The fixed effect parameters are denoted by
 20 $\{\beta_0, \dots, \beta_5\}$, and $\{b_{0i}, \dots, b_{4i}\}$ are the patient specific random effects. The
 21 random effects follow a multivariate normal distribution with mean zero and
 22 variance-covariance matrix \mathbf{W} . The error $\varepsilon_i(t)$ is assumed to be t-distributed
 23 with three degrees of freedom (see Appendix B.1) and scale σ , and is inde-
 24 pendent of the random effects.

To model the impact of PSA measurements on the risk of upgrading, our joint model uses a relative risk sub-model. More specifically, the hazard of upgrading denoted as $h_i(t)$, and the cumulative-risk of upgrading denoted as $R_i(t)$, at a time t are (see Panel C, Figure 1):

$$\begin{aligned} h_i(t) &= h_0(t) \exp \left(\gamma \text{age}_i + \alpha_1 m_i(t) + \alpha_2 \frac{dm_i(t)}{dt} \right), \\ R_i(t) &= \exp \left\{ - \int_0^t h_i(s) ds \right\}, \end{aligned} \quad (2)$$

where, γ is the parameter for the effect of age. The impact of PSA on the hazard of upgrading is modeled in two ways, namely the impact of the error

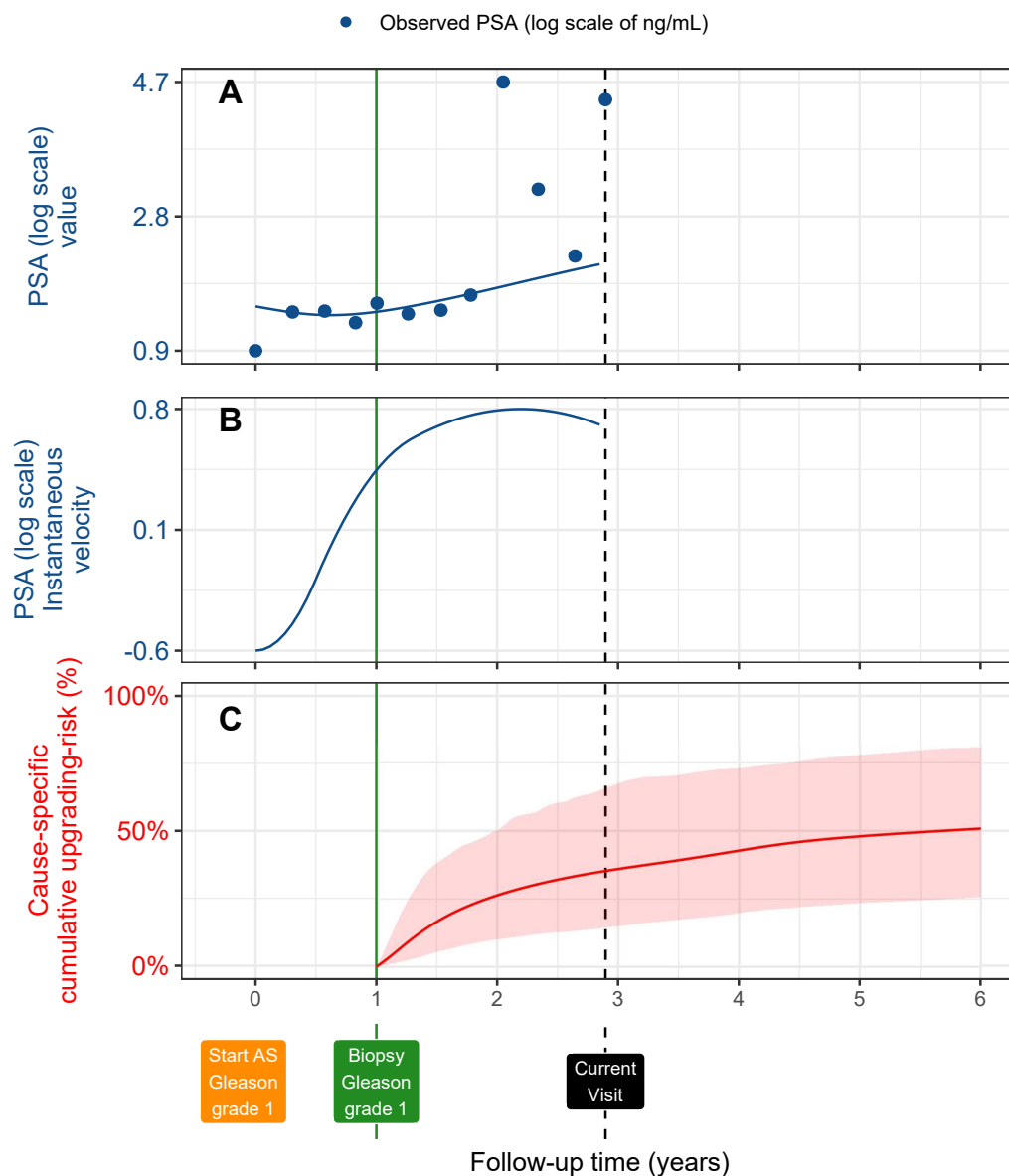


Figure 1: **Illustration of the joint model on a real PRIAS dataset patient.** **Panel A:** Observed (blue dots) and fitted PSA (solid blue line) measurements, log-transformed. **Panel B:** Estimated instantaneous velocity of PSA (log-transformed). **Panel C:** Predicted cumulative-risk of upgrading (95% credible interval shaded). Upgrading is defined as increase in Gleason grade group [1] from grade group 1 to 2 or higher. This risk of upgrading is available starting from the time of the latest negative biopsy (vertical green line at year 1 of follow-up). Joint model estimated it by combining the fitted PSA value and velocity (both on log scale of PSA) and time of latest negative biopsy. Black dashed line at year 4 denotes time of current visit.

free underlying PSA value $m_i(t)$ (see Panel A, Figure 1), and the impact of the underlying PSA velocity $dm_i(t)/dt$ (see Panel B, Figure 1). The corresponding parameters are α_1 and α_2 , respectively. Lastly, $h_0(t)$ is the baseline hazard at time t , and is modeled flexibly using P-splines [5]. More specifically:

$$\log h_0(t) = \gamma_{h_0,0} + \sum_{q=1}^Q \gamma_{h_0,q} B_q(t, \mathbf{v}),$$

25 where $B_q(t, \mathbf{v})$ denotes the q -th basis function of a B-spline with knots $\mathbf{v} =$
 26 v_1, \dots, v_Q and vector of spline coefficients γ_{h_0} . To avoid choosing the number
 27 and position of knots in the spline, a relatively high number of knots (e.g.,
 28 15 to 20) are chosen and the corresponding B-spline regression coefficients
 29 γ_{h_0} are penalized using a differences penalty [5].

We estimate the parameters of the joint model using Markov chain Monte Carlo (MCMC) methods under the Bayesian framework. Let $\boldsymbol{\theta}$ denote the vector of all of the parameters of the joint model. The joint model postulates that given the random effects, the time of upgrading, and the PSA measurements taken over time are all mutually independent. Under this assumption the posterior distribution of the parameters is given by:

$$\begin{aligned} p(\boldsymbol{\theta}, \mathbf{b} \mid \mathcal{A}_n) &\propto \prod_{i=1}^n p(l_i, r_i, \mathbf{y}_i \mid \mathbf{b}_i, \boldsymbol{\theta}) p(\mathbf{b}_i \mid \boldsymbol{\theta}) p(\boldsymbol{\theta}) \\ &\propto \prod_{i=1}^n p(l_i, r_i \mid \mathbf{b}_i, \boldsymbol{\theta}) p(\mathbf{y}_i \mid \mathbf{b}_i, \boldsymbol{\theta}) p(\mathbf{b}_i \mid \boldsymbol{\theta}) p(\boldsymbol{\theta}), \\ p(\mathbf{b}_i \mid \boldsymbol{\theta}) &= \frac{1}{\sqrt{(2\pi)^q \det(\mathbf{W})}} \exp \left\{ -\frac{1}{2} (\mathbf{b}_i^T \mathbf{W}^{-1} \mathbf{b}_i) \right\}, \end{aligned}$$

where, the likelihood contribution of the PSA outcome, conditional on the random effects is:

$$p(\mathbf{y}_i \mid \mathbf{b}_i, \boldsymbol{\theta}) = \frac{1}{(\sqrt{2\pi}\sigma^2)^{n_i}} \exp \left\{ -\frac{\sum_{j=1}^{n_i} (y_{ij} - m_{ij})^2}{2\sigma^2} \right\},$$

where n_i is the number of PSA measurements of the i -th patient. The likelihood contribution of the time of upgrading outcome is given by:

$$p(l_i, r_i \mid \mathbf{b}_i, \boldsymbol{\theta}) = \exp \left\{ -\int_0^{l_i} h_i(s) ds \right\} - \exp \left\{ -\int_0^{r_i} h_i(s) ds \right\}. \quad (3)$$

30 The integrals in (3) do not have a closed-form solution, and therefore we use
 31 a 15-point Gauss-Kronrod quadrature rule to approximate them.

32 We use independent normal priors with zero mean and variance 100 for
 33 the fixed effects $\{\beta_0, \dots, \beta_5\}$, and inverse Gamma prior with shape and rate
 34 both equal to 0.01 for the parameter σ^2 . For the variance-covariance matrix
 35 \mathbf{W} of the random effects we take inverse Wishart prior with an identity scale
 36 matrix and degrees of freedom equal to 5 (number of random effects). For
 37 the relative risk model's parameter γ and the association parameters α_1, α_2 ,
 38 we use independent normal priors with zero mean and variance 100.

39 *Appendix A.1. Assumption of t-distributed (df=3) Error Terms*

40 With regards to the choice of the distribution for the error term ε for
 41 the PSA measurements (see Equation 1), we attempted fitting multiple joint
 42 models differing in error distribution, namely t-distribution with three, and
 43 four degrees of freedom, and a normal distribution for the error term. How-
 44 ever, the model assumption for the error term were best met by the model
 45 with t-distribution having three degrees of freedom. The quantile-quantile
 46 plot of subject-specific residuals for the corresponding model in Panel A of
 47 Figure 2, shows that the assumption of t-distributed (df=3) errors is reason-
 48 ably met by the fitted model.

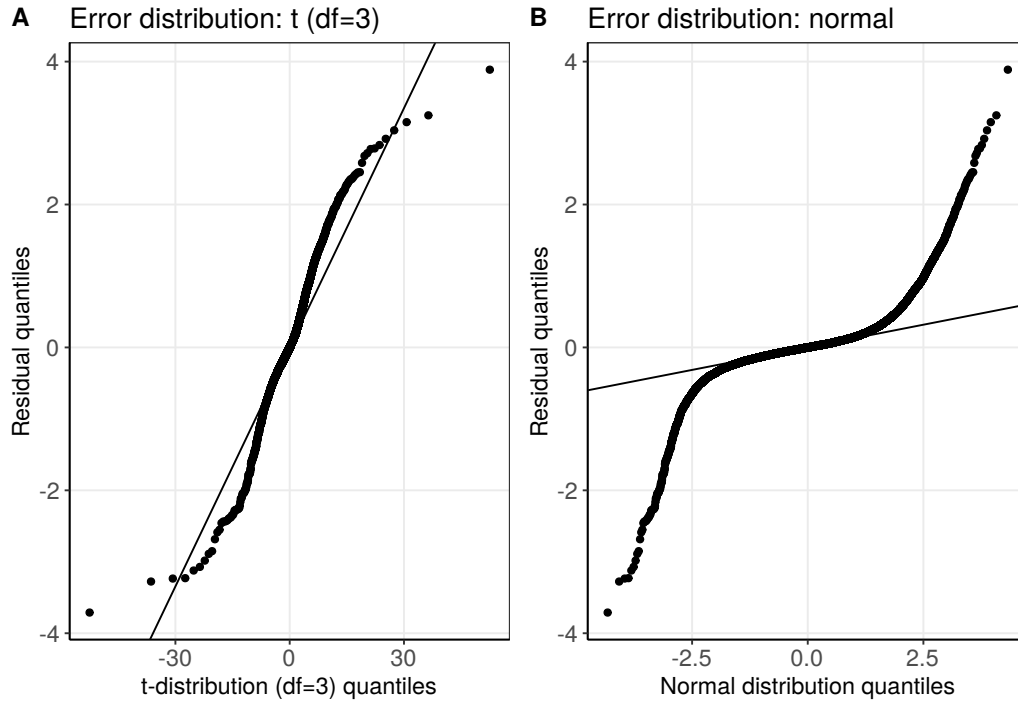


Figure 2: **Quantile-quantile plot** of subject-specific PSA residuals from two different joint models fitted to the PRIAS dataset. **Panel A:** model assuming a t-distribution ($df=3$) for the error term ε (see Equation 1). **Panel B:** model assuming a normal distribution for the error term ε . We selected the model with t-distributed error terms.

49 *Appendix A.2. Results*

50 Characteristics of the six validation cohorts from the GAP3 database [6]
 51 are shown in Table 1, Table 2, and Table 3. The cause-specific cumulative
 52 upgrading-risk in these cohorts is shown in Figure 3.

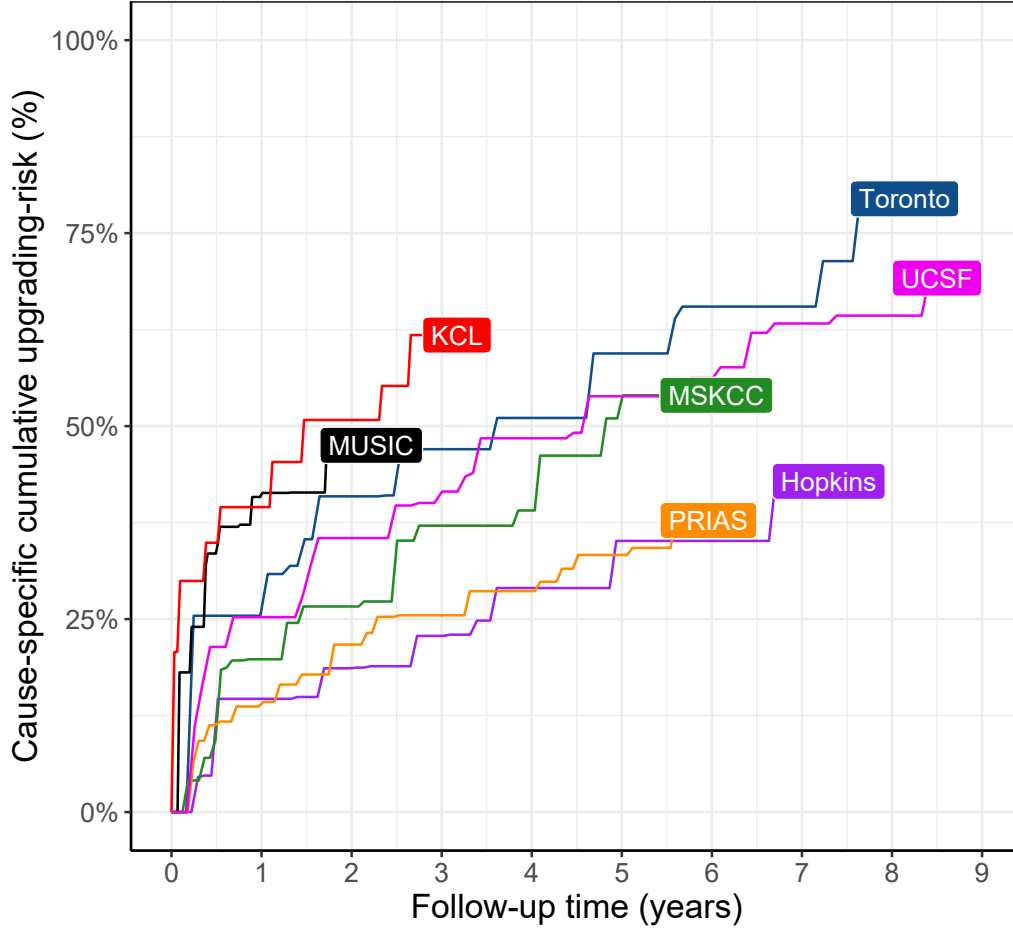


Figure 3: **Nonparametric estimate [7] of the cause-specific cumulative upgrading-risk** in the world’s largest AS cohort PRIAS, and largest six AS cohorts from the GAP3 database [6]. Abbreviations are *Hopkins*: Johns Hopkins Active Surveillance, *PRIAS*: Prostate Cancer International Active Surveillance, *Toronto*: University of Toronto Active Surveillance, *MSKCC*: Memorial Sloan Kettering Cancer Center Active Surveillance, *KCL*: King’s College London Active Surveillance, *MUSIC*: Michigan Urological Surgery Improvement Collaborative AS, *UCSF*: University of California San Francisco Active Surveillance.

Table 1: **Summary of the Hopkins and Toronto validation cohorts from the GAP3 database [6]**. The primary event of interest is upgrading, that is, increase in Gleason grade group from group 1 to 2 or higher. #PSA: number of PSA, #biopsies: number of biopsies, IQR: interquartile range, PSA: prostate-specific antigen. Full names of cohorts are *Hopkins*: Johns Hopkins Active Surveillance, *Toronto*: University of Toronto Active Surveillance

Characteristic	Hopkins	Toronto
Total patients	1392	1046
Upgrading (primary event)	260	359
Median age (years)	62 (IQR: 66–69)	67 (IQR: 60–72)
Median maximum follow-up per patient (years)	3 (IQR: 1.3–5.8)	4.5 (IQR: 1.9–8.4)
Total PSA measurements	11126	13984
Median #PSA per patient	6 (IQR: 4–11)	12 (IQR: 7–19)
Median PSA (ng/mL)	4.7 (IQR: 2.9–6.7)	6 (IQR: 3.7–9.0)
Total biopsies	1926	909
Median #biopsies per patient	1 (IQR: 1–2)	1 (IQR: 1–2)

Table 2: **Summary of the MSKCC and UCSF validation cohorts from the GAP3 database [6]**. The primary event of interest is upgrading, that is, increase in Gleason grade group from group 1 to 2 or higher. #PSA: number of PSA, #biopsies: number of biopsies, IQR: interquartile range, PSA: prostate-specific antigen. Full names of cohorts are *MSKCC*: Memorial Sloan Kettering Cancer Center Active Surveillance, *UCSF*: University of California San Francisco Active Surveillance.

Characteristic	MSKCC	UCSF
Total patients	894	1397
Upgrading (primary event)	242	547
Median age (years)	63 (IQR: 57–68)	63 (IQR: 57–68)
Median maximum follow-up per patient (years)	5.3 (IQR: 1.8–8.3)	3.6 (IQR: 1.5–7.2)
Total PSA measurements	10704	16093
Median #PSA per patient	11 (IQR: 5–17)	8 (IQR: 4–16)
Median PSA (ng/mL)	4.7 (IQR: 2.8–7.1)	5.0 (IQR: 3.4–7.2)
Total biopsies	1102	3512
Median #biopsies per patient	1 (IQR: 1–2)	2 (IQR: 2–3)

Table 3: **Summary of the MUSIC and KCL validation cohorts from the GAP3 database [6].** The primary event of interest is upgrading, that is, increase in Gleason grade group from group 1 to 2 or higher. #PSA: number of PSA, #biopsies: number of biopsies, IQR: interquartile range, PSA: prostate-specific antigen. Full names of cohorts are *KCL*: King’s College London Active Surveillance, *MUSIC*: Michigan Urological Surgery Improvement Collaborative AS.

Characteristic	MUSIC	KCL
Total patients	2743	616
Upgrading (primary event)	385	198
Median age (years)	65 (IQR: 60–71)	63 (IQR: 58–68)
Median maximum follow-up per patient (years)	1.2 (IQR: 0.6–2.2)	2.4 (IQR: 1.3–3.8)
Total PSA measurements	12087	2987
Median #PSA per patient	4 (IQR: 2–6)	4 (IQR: 2–6)
Median PSA (ng/mL)	5.1 (IQR: 3.4–7.1)	6 (IQR: 4–9)
Total biopsies	1032	484
Median #biopsies per patient	1 (IQR: 1–1)	1 (IQR: 1–1)

Table 4: **Estimated variance-covariance matrix \mathbf{W}** of the random effects $\mathbf{b} = (b_0, b_1, b_2, b_3, b_4)$ from the joint model fitted to the PRIAS dataset. The variances of the random effects are highlighted along the diagonal of the variance-covariance matrix.

Random Effects	b_0	b_1	b_2	b_3	b_4
b_0	0.229	0.030	0.023	0.073	0.007
b_1	0.030	0.149	0.098	0.171	0.085
b_2	0.023	0.098	0.276	0.335	0.236
b_3	0.073	0.171	0.335	0.560	0.359
b_4	0.007	0.085	0.236	0.359	0.351

The joint model was fitted using the R package **JMbayes** [8]. This package utilizes the Bayesian methodology to estimate model parameters. The corresponding posterior parameter estimates are shown in Table 5 (longitudinal sub-model for PSA outcome) and Table 6 (relative risk sub-model). The parameter estimates for the variance-covariance matrix \mathbf{W} from the longitudinal sub-model for PSA are shown in the following Table 4:

For the PSA mixed effects sub-model parameter estimates (see Equation 1), in Table 5 we can see that the age of the patient trivially affects the baseline $\log_2(\text{PSA} + 1)$ measurement. Since the longitudinal evolution of $\log_2(\text{PSA} + 1)$ measurements is modeled with non-linear terms, the interpretation of the coefficients corresponding to time is not straightforward. In lieu of the interpretation, in Figure 4 we present plots of observed versus fitted

Table 5: **Parameters of the longitudinal sub-model:** Estimated mean and 95% credible interval for parameters in Equation (1).

Variable	Mean	Std. Dev	2.5%	97.5%	P
Intercept	2.129	0.060	2.009	2.244	<0.001
Age	0.008	0.001	0.007	0.010	<0.001
Spline: [0.0, 0.5] years	0.063	0.007	0.051	0.075	<0.001
Spline: [0.5, 1.3] years	0.196	0.010	0.177	0.217	<0.001
Spline: [1.3, 3.0] years	0.244	0.014	0.217	0.272	<0.001
Spline: [3.0, 6.3] years	0.382	0.014	0.356	0.410	<0.001
σ	0.139	0.001	0.138	0.140	

Table 6: **Parameters of the relative risk sub-model:** Estimated mean and 95% credible interval for the parameters in Equation (2).

Variable	Mean	Std. Dev	2.5%	97.5%	P
Age	0.037	0.006	0.025	0.049	<0.001
Fitted $\log_2(\text{PSA} + 1)$ value	-0.012	0.076	-0.164	0.135	0.856
Fitted $\log_2(\text{PSA} + 1)$ velocity	2.266	0.299	1.613	2.767	<0.001

65 PSA profiles for nine randomly selected patients.

66 For the relative risk sub-model (see Equation 2), the parameter estimates
 67 in Table 6 show that $\log_2(\text{PSA} + 1)$ velocity and age of the patient were
 68 significantly associated with the hazard of upgrading.

69 It is important to note that since age, and $\log_2(\text{PSA} + 1)$ value and ve-
 70 locity are all measured on different scales, a comparison between the cor-
 71 responding parameter estimates is not easy. To this end, in Table 7, we
 72 present the hazard ratio of upgrading, for an increase in the aforementioned
 73 variables from their 25-th to the 75-th percentile. For example, an increase
 74 in fitted $\log_2(\text{PSA} + 1)$ velocity from -0.085 to 0.308 (fitted 25-th and 75-th
 75 percentiles) corresponds to a hazard ratio of 2.433. The interpretation for
 76 the rest is similar.

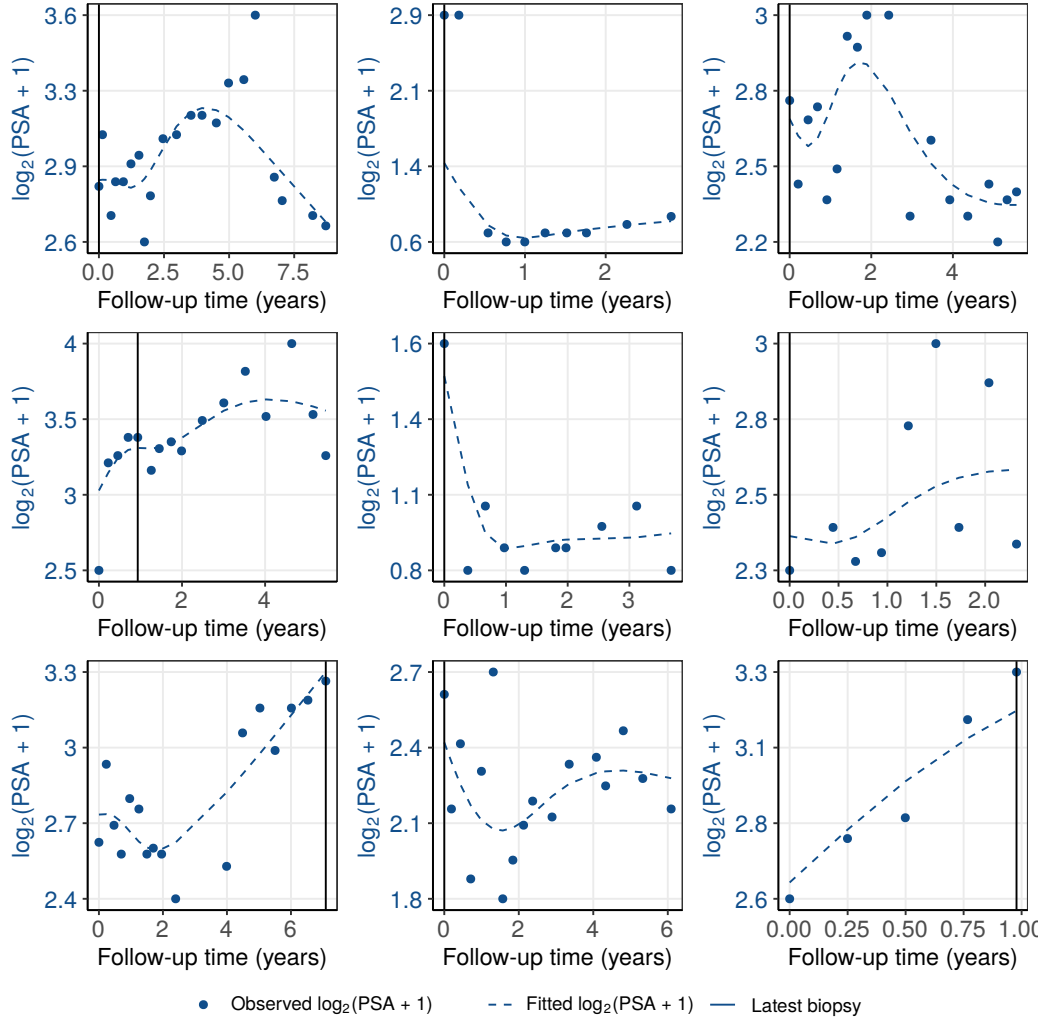


Figure 4: **Fitted versus observed $\log_2(\text{PSA} + 1)$ profiles** for nine randomly selected PRIAS patients. The fitted profiles utilize information from the observed PSA measurements, and time of the latest biopsy.

Table 7: **Hazard ratio and 95% credible interval (CI) for upgrading:** Variables are on different scale and hence we compare an increase in the variables of relative risk sub-model from their 25-th percentile (P_{25}) to their 75-th percentile (P_{75}). Except for age, quartiles for all other variables are based on their fitted values obtained from the joint model fitted to the PRIAS dataset.

Variable	P_{25}	P_{75}	Hazard ratio [95% CI]
Age	61	71	1.455 [1.285, 1.631]
Fitted $\log_2(\text{PSA} + 1)$ value	2.360	3.078	0.991 [0.889, 1.102]
Fitted $\log_2(\text{PSA} + 1)$ velocity	-0.085	0.308	2.433 [1.883, 2.962]

Table 8: **Parameters of the relative risk sub-model in validation cohorts.** We fitted separate joint models for each of the six GAP3 validation cohorts as well. The specification of these joint models was same as that of the model for PRIAS. Two important predictors in the relative-risk sub-model, namely, the $\log_2(\text{PSA} + 1)$ value and velocity have different impact on upgrading-risk across the cohorts. Table shows the mean estimate of these parameters with 95% credible interval in brackets. Strongest average effect of $\log_2(\text{PSA} + 1)$ velocity is in PRIAS cohort, whereas the weakest is in KCL cohort. The strongest average effect of $\log_2(\text{PSA} + 1)$ value is in the Toronto cohort whereas the weakest is in PRIAS cohort. Full names of cohorts are *Hopkins*: Johns Hopkins Active Surveillance, *PRIAS*: Prostate Cancer International Active Surveillance, *Toronto*: University of Toronto Active Surveillance, *MSKCC*: Memorial Sloan Kettering Cancer Center Active Surveillance, *KCL*: King's College London Active Surveillance, *MUSIC*: Michigan Urological Surgery Improvement Collaborative AS, *UCSF*: University of California San Francisco Active Surveillance.

Cohort	Fitted $\log_2(\text{PSA} + 1)$ value	Fitted $\log_2(\text{PSA} + 1)$ velocity
PRIAS	-0.012 [-0.164, 0.135]	2.266 [1.613, 2.767]
Hopkins	0.061 [-0.323, 0.329]	1.839 [0.761, 4.378]
MSKCC	0.336 [0.081, 0.583]	1.122 [0.421, 1.980]
Toronto	0.572 [0.347, 0.794]	0.943 [0.464, 1.554]
UCSF	0.498 [0.326, 0.673]	0.812 [0.280, 1.383]
MUSIC	0.441 [0.092, 0.767]	0.029 [-0.552, 0.512]
KCL	0.194 [-0.104, 0.540]	0.840 [-0.087, 1.665]

77 Appendix B. Risk Predictions for Upgrading

Let us assume a new patient j , for whom we need to estimate the upgrading-risk. Let his current follow-up visit time be v , latest time of biopsy be t , observed vector PSA measurements be $\mathcal{Y}_j(v)$. The combined information from the observed data about the time of upgrading, is given by the following posterior predictive distribution $g(T_j^*)$ of his time T_j^* of upgrading:

$$\begin{aligned} g(T_j^*) &= p\{T_j^* \mid T_j^* > t, \mathcal{Y}_j(v), \mathcal{A}_n\} \\ &= \int \int p(T_j^* \mid T_j^* > t, \mathbf{b}_j, \boldsymbol{\theta}) p\{\mathbf{b}_j \mid T_j^* > t, \mathcal{Y}_j(v), \boldsymbol{\theta}\} p(\boldsymbol{\theta} \mid \mathcal{A}_n) d\mathbf{b}_j d\boldsymbol{\theta}. \end{aligned}$$

78 The distribution $g(T_j^*)$ depends not only depends on the observed data of the
 79 patient $T_j^* > t, \mathcal{Y}_j(v)$, but also depends on the information from the PRIAS
 80 dataset \mathcal{A}_n . To this the the posterior distribution of random effects \mathbf{b}_j and
 81 posterior distribution of the vector of all parameters $\boldsymbol{\theta}$ are utilized, respec-
 82 tively. The distribution $g(T_j^*)$ can be estimated as detailed in Rizopoulos
 83 et al. [9]. Since, many prostate cancer patients may not obtain upgrading
 84 in the current follow-up period of PRIAS, $g(T_j^*)$ can only be estimated for a
 85 currently limited follow-up period.

The cause-specific cumulative upgrading-risk can be derived from $g(T_j^*)$ as given in [9]. It is given by:

$$R_j(u \mid t, v) = \Pr\{T_j^* > u \mid T_j^* > t, \mathcal{Y}_j(v), \mathcal{A}_n\}, \quad u \geq t. \quad (4)$$

86 The personalized risk profile of the patient (see Panel C, Figure 5) updates
 87 as more data is gathered over follow-up visits.

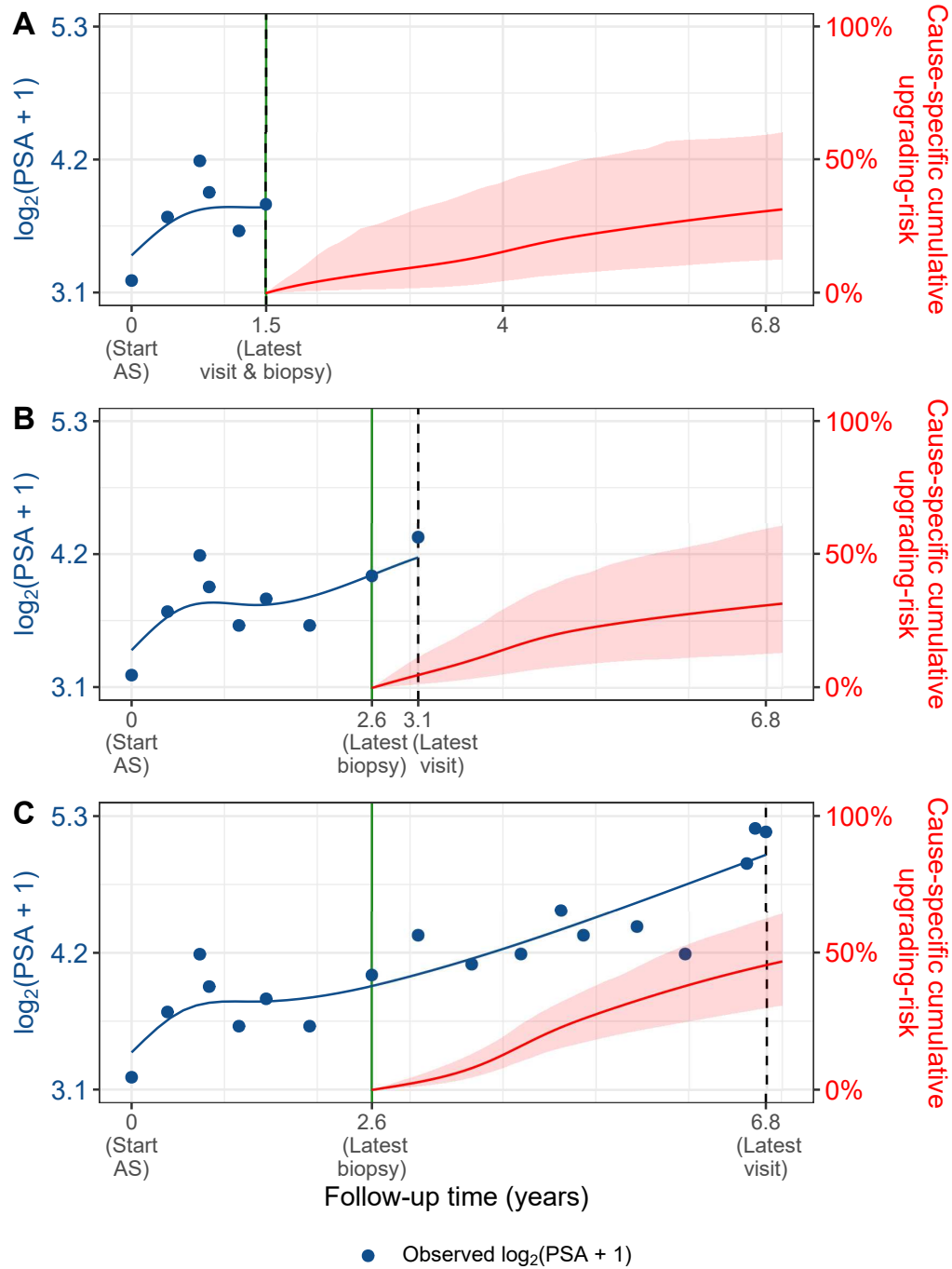


Figure 5: **Cause-specific cumulative upgrading-risk changing dynamically over follow-up** as more patient data is gathered. The three **Panels A,B and C**: are ordered by the time of the latest visit (dashed vertical black line) of a new patient. At each of the latest follow-up visits, we combine the accumulated PSA measurements (shown in blue), and latest time of negative biopsy (solid vertical green line) to obtain the updated cumulative-risk profile (shown in red) of the patient.

88 *Appendix B.1. Validation of Risk Predictions*

89 We wanted to check the usefulness of our model for not only the PRIAS
 90 patients but also for patients from other cohorts. To this end, we validated
 91 our model in the PRIAS dataset (internal validation) and in largest six co-
 92 horts from the GAP3 database [6]. These are the University of Toronto AS
 93 (Toronto), Johns Hopkins AS (Hopkins), Memorial Sloan Kettering Can-
 94 cer Center AS (MSKCC), University of California San Francisco Active
 95 Surveillance (UCSF), King’s College London AS (KCL), Michigan Urological
 96 Surgery Improvement Collaborative AS (MUSIC).

Calibration-in-the-large We first assessed calibration-in-the-large [10]
 of our model in the aforementioned cohorts. To this end, we used our model
 to predict the cause-specific cumulative upgrading-risk for each patient given
 their PSA measurements and biopsy results. We then averaged the resulting
 profiles of cause-specific cumulative upgrading-risk. Subsequently we com-
 pared the averaged cumulative-risk profile with a non-parametric estimate [7]
 of the cause-specific cumulative upgrading-risk in each of the cohorts. The
 results are shown in Panel A of Figure 6. We can see that our model’s cali-
 bration is fine only in PRIAS and Hopkins cohorts. To improve our model’s
 calibration in KCL, MUSIC, Toronto, and MSKCC cohorts, we recalibrated
 the baseline hazard of the joint model fitted to the PRIAS dataset, indi-
 vidually for each of these cohorts. More specifically, given the data of an
 external cohort \mathcal{A}_n^c , where c denotes the cohort, the recalibrated parameters
 γ_{h0}^c (Appendix A) of the log baseline hazard are given by:

$$p(\gamma_{h0}^c \mid \mathcal{A}_n^c, \mathbf{b}^c, \boldsymbol{\theta}) \propto \prod_{i=1}^{n^c} p(l_i^c, r_i^c \mid \mathbf{b}_i^c, \boldsymbol{\theta}) p(\gamma_{h0}^c) \quad (5)$$

97 where n^c are the number of patients in the c -th cohort and $\boldsymbol{\theta}$ are the pa-
 98 rameters of the joint model fitted to the PRIAS dataset. The interval in
 99 which upgrading is observed for the i – th patient is given by l_i^c, r_i^c , with
 100 $r_i^c = \infty$ for right censored patients. The symbol \mathbf{b}_i^c denotes patient-specific
 101 random effects (Appendix A). The random effects are obtained using the joint
 102 model fitted to the PRIAS dataset prior to recalibration. We re-evaluated the
 103 calibration-in-the-large of our model after the recalibration of the baseline
 104 hazard individually for each cohort. The improved calibration-in-the-large is
 105 shown in Panel B of Figure 6.

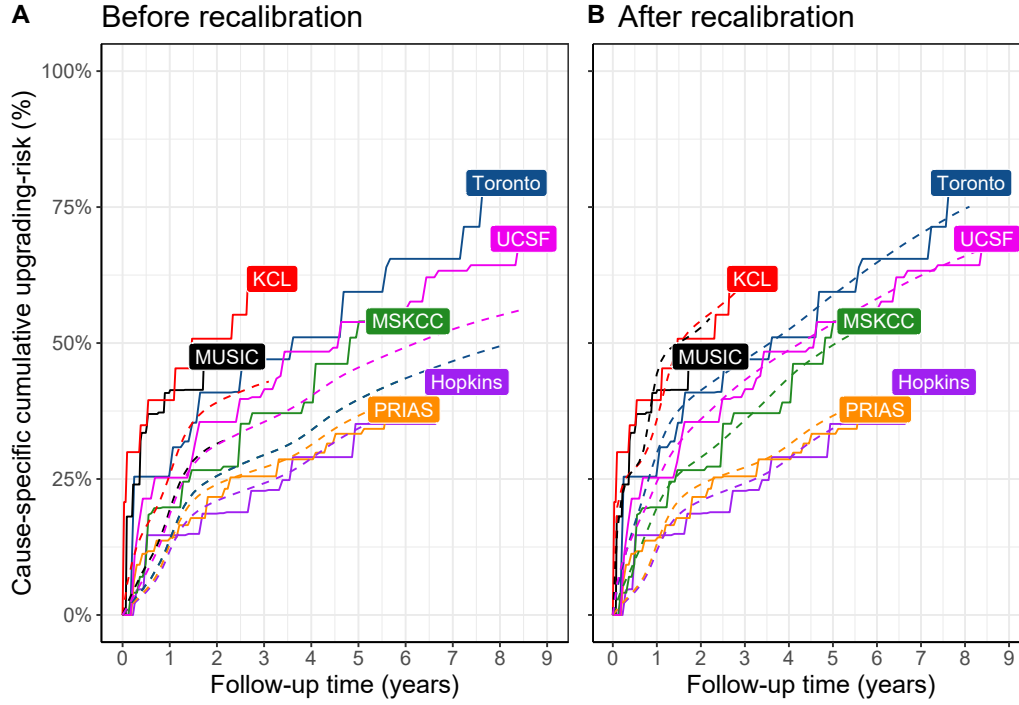


Figure 6: **Calibration-in-the-large of our model:** In **Panel A** we can see that our model is not well calibrated for use in KCL, MUSIC, Toronto and MSKCC. In **Panel B** we can see that calibration of model predictions improved in KCL, MUSIC, Toronto and MSKCC cohorts after recalibrating our model. Recalibration was not necessary for Hopkins cohort. Full names of Cohorts are *PRIAS*: Prostate Cancer International Active Surveillance, *Toronto*: University of Toronto Active Surveillance, *Hopkins*: Johns Hopkins Active Surveillance, *MSKCC*: Memorial Sloan Kettering Cancer Center Active Surveillance, *KCL*: King's College London Active Surveillance, *MUSIC*: Michigan Urological Surgery Improvement Collaborative Active Surveillance, *UCSF*: University of California San Francisco Active Surveillance.

106 ***Recalibrated PRIAS Model Versus Individual Joint Models***
107 ***For Each Cohort*** We wanted to check if our recalibrated PRIAS model
108 performed as good as a new joint model that could be fitted to the external
109 cohorts. To this end, we predicted cause-specific cumulative upgrading-risk
110 for each patient from each cohort using two sets of models, namely the recal-
111 ibrated PRIAS model for each cohort, and a new joint model fitted to each
112 cohort. The difference in predicted cause-specific cumulative upgrading-risk
113 from these models is shown in Figure 7. We can see that the difference is
114 smaller in those cohorts in which the effects of $\log_2(\text{PSA} + 1)$ value and ve-
115 locity were similar to that of PRIAS (Table 8). For example, the Hopkins
116 cohort had parameter estimates similar to that of PRIAS and consequently
117 the difference in predicted risks for this cohort is smallest. The opposite of
118 this phenomenon holds true for the MUSIC and KCL cohorts.

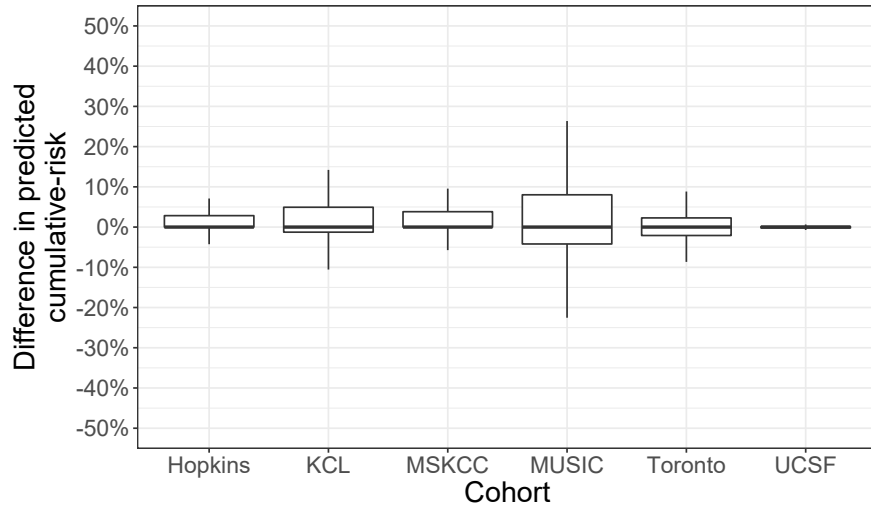


Figure 7: **Comparison of predictions from recalibrated PRIAS model with individual joint models fitted to external cohorts:** On Y-axis we show the difference between predicted cause-specific cumulative upgrading-risk for individual patients using two models, namely the recalibrated PRIAS model for each cohort, and individual joint model fitted to each cohort. The figure shows that the difference is smaller in those cohorts in which the effects of $\log_2(\text{PSA} + 1)$ value and velocity were similar to that of PRIAS (Table 8). Full names of Cohorts are *PRIAS*: Prostate Cancer International Active Surveillance, *Toronto*: University of Toronto Active Surveillance, *Hopkins*: Johns Hopkins Active Surveillance, *MSKCC*: Memorial Sloan Kettering Cancer Center Active Surveillance, *KCL*: King’s College London Active Surveillance, *MUSIC*: Michigan Urological Surgery Improvement Collaborative Active Surveillance, *UCSF*: University of California San Francisco Active Surveillance.

Validation of Dynamic Cumulative-Risk Predictions As shown in Figure 5 the cumulative-risk predictions from the joint model are dynamic in nature. That is, they update as more data becomes available over time. Consequently, the discrimination and calibration of the joint model also depends on the available data. We assessed these two measures dynamically in the PRIAS cohort (interval validation) and in the largest six external cohorts that are part of the GAP3 database. For discrimination we utilized the time-varying area under the receiver operating characteristic curve or time-varying AUC [9]. For time-varying calibration we assessed the mean absolute prediction error or MAPE [9]. The AUC indicates how well the model discriminates between patients who experience upgrading and those do not. The MAPE indicates how accurately the model predicts upgrading. Both AUC and MAPE are restricted to $[0, 1]$. However, it is preferred that $\text{AUC} > 0.5$ because an $\text{AUC} \leq 0.5$ indicates that the model performs worse than random discrimination. Ideally MAPE should be 0.

We calculate AUC and MAPE in a time-dependent manner. More specifically, given the time of latest biopsy t , and history of PSA measurements up to time v , we calculate AUC and MAPE for a medically relevant time frame $(t, v]$, within which the occurrence of upgrading is of interest. In the case of prostate cancer, at any point in time v it is of interest to identify patients who may have experienced upgrading in the last one year $(v - 1, v]$. That is we set $t = v - 1$. We then calculate AUC and MAPE at a gap of every six months (follow-up schedule of PRIAS). That is, $v \in \{1, 1.5, \dots\}$ years. To obtain reliable estimates of AUC and MAPE, in each cohort we restrict v to a maximum time point v_{\max} , such that there are at least 10 patients who experience upgrading after v_{\max} . This maximum time point v_{\max} differs between cohorts, and is given in Table 9.

The results for estimates of AUC and MAPE are summarized in Figure 8, and in Table 10 to Table 16. Results are based on the recalibrated PRIAS model for the GAP3 cohorts. The results show that AUC remains more or less constant in all cohorts as more data becomes available for patients. The AUC obtains a moderate value, roughly between 0.5 and 0.7 for all cohorts. On the other hand, MAPE reduces by a big margin after year two of follow-up. This could be because of two reasons. Firstly, MAPE at year one is based only on four PSA measurements gathered in first year of follow-up, whereas after year two number of PSA measurements increase. Secondly, patients in year one consist of two sub-populations, namely patients with a correct Gleason grade group 1 at the time of inclusion in AS, and patients

Table 9: **Maximum follow-up period up to which we can reliably predict upgrading-risk.** In each cohort, this time point is chosen such that there are at least 10 patients who experience upgrading after this time point. Full names of Cohorts are *PRIAS*: Prostate Cancer International Active Surveillance, *Toronto*: University of Toronto Active Surveillance, *Hopkins*: Johns Hopkins Active Surveillance, *MSKCC*: Memorial Sloan Kettering Cancer Center Active Surveillance, *KCL*: King's College London Active Surveillance, *MUSIC*: Michigan Urological Surgery Improvement Collaborative Active Surveillance, *UCSF*: University of California San Francisco Active Surveillance.

Cohort	Maximum Prediction Time (years)
PRIAS	6
KCL	3
MUSIC	2
Toronto	8
MSKCC	6
Hopkins	7
UCSF	8.5

157 who probably had Gleason grade group 2 at inclusion but were misclassified
 158 by the urologist as Gleason grade group 1 patients. To remedy this problem,
 159 a biopsy for all patients at year one is commonly recommended in all AS
 160 programs [11].

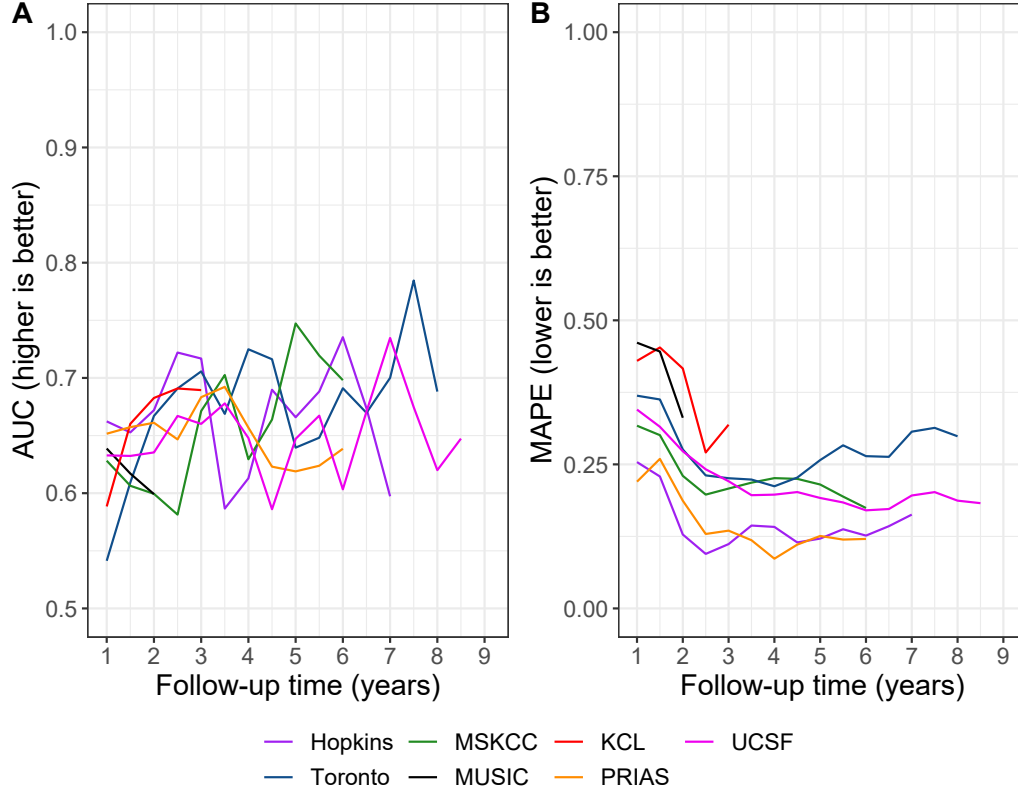


Figure 8: **Validation of dynamic predictions of cause-specific cumulative upgrading-risk.** In **Panel A** we can see that the time dependent area under the receiver operating characteristic curve or AUC (measure of discrimination) is above 0.5 in PRIAS (internal validation), and in Toronto, Hopkins, MSKCC, KCL, and MUSIC AS cohorts (external validation). In **Panel B** we can see that the time dependent root mean squared prediction error or MAPE (measure of calibration) is similar for PRIAS and Hopkins cohorts. The bootstrapped 95% confidence interval for these estimates are presented in Table 10 to Table 15. Full names of Cohorts are *PRIAS*: Prostate Cancer International Active Surveillance, *Toronto*: University of Toronto Active Surveillance, *Hopkins*: Johns Hopkins Active Surveillance, *MSKCC*: Memorial Sloan Kettering Cancer Center Active Surveillance, *KCL*: King's College London Active Surveillance, *MUSIC*: Michigan Urological Surgery Improvement Collaborative Active Surveillance, *UCSF*: University of California San Francisco Active Surveillance.

Table 10: **Internal validation of predictions of upgrading in PRIAS cohort.** The area under the receiver operating characteristic curve or AUC (measure of discrimination) and mean absolute prediction error or MAPE (measure of calibration) are calculated over the follow-up period at a gap of 6 months. In addition bootstrapped 95% confidence intervals (CI) are also presented.

Follow-up period (years)	AUC (95% CI)	MAPE (95%CI)
0.0 to 1.0	0.652 [0.611, 0.690]	0.220 [0.214, 0.227]
0.5 to 1.5	0.657 [0.641, 0.673]	0.260 [0.254, 0.265]
1.0 to 2.0	0.661 [0.647, 0.678]	0.187 [0.183, 0.191]
1.5 to 2.5	0.647 [0.596, 0.688]	0.129 [0.122, 0.140]
2.0 to 3.0	0.683 [0.642, 0.723]	0.135 [0.125, 0.146]
2.5 to 3.5	0.692 [0.632, 0.748]	0.118 [0.111, 0.128]
3.0 to 4.0	0.657 [0.603, 0.709]	0.086 [0.080, 0.092]
3.5 to 4.5	0.623 [0.582, 0.660]	0.111 [0.105, 0.116]
4.0 to 5.0	0.619 [0.582, 0.654]	0.126 [0.118, 0.131]
4.5 to 5.5	0.624 [0.537, 0.711]	0.119 [0.103, 0.135]
5.0 to 6.0	0.639 [0.582, 0.696]	0.121 [0.103, 0.138]

Table 11: **External validation of predictions of upgrading in University of Toronto Active Surveillance cohort.** The area under the receiver operating characteristic curve or AUC (measure of discrimination) and mean absolute prediction error or MAPE (measure of calibration) are calculated over the follow-up period at a gap of 6 months. In addition bootstrapped 95% confidence intervals (CI) are also presented.

Follow-up period (years)	AUC (95% CI)	MAPE (95%CI)
0.0 to 1.0	0.541 [0.470, 0.621]	0.369 [0.352, 0.381]
0.5 to 1.5	0.609 [0.547, 0.661]	0.363 [0.348, 0.376]
1.0 to 2.0	0.667 [0.634, 0.712]	0.276 [0.259, 0.296]
1.5 to 2.5	0.691 [0.651, 0.730]	0.231 [0.205, 0.254]
2.0 to 3.0	0.706 [0.637, 0.762]	0.226 [0.196, 0.260]
2.5 to 3.5	0.669 [0.586, 0.741]	0.224 [0.195, 0.258]
3.0 to 4.0	0.725 [0.649, 0.806]	0.212 [0.184, 0.238]
3.5 to 4.5	0.716 [0.642, 0.793]	0.227 [0.206, 0.258]
4.0 to 5.0	0.640 [0.579, 0.717]	0.257 [0.222, 0.312]
4.5 to 5.5	0.648 [0.579, 0.740]	0.283 [0.247, 0.326]
5.0 to 6.0	0.691 [0.608, 0.793]	0.264 [0.232, 0.302]
5.5 to 6.5	0.670 [0.543, 0.776]	0.263 [0.227, 0.307]
6.0 to 7.0	0.700 [0.544, 0.851]	0.307 [0.258, 0.363]
6.5 to 7.5	0.785 [0.640, 0.866]	0.313 [0.272, 0.360]
7.0 to 8.0	0.688 [0.532, 0.786]	0.299 [0.249, 0.361]

Table 12: **External validation of predictions of upgrading in University of California San Francisco Active Surveillance cohort.** The area under the receiver operating characteristic curve or AUC (measure of discrimination) and mean absolute prediction error or MAPE (measure of calibration) are calculated over the follow-up period at a gap of 6 months. In addition bootstrapped 95% confidence intervals (CI) are also presented.

Follow-up period (years)	AUC (95% CI)	MAPE (95%CI)
0.0 to 1.0	0.633 [0.585, 0.674]	0.345 [0.337, 0.357]
0.5 to 1.5	0.632 [0.599, 0.673]	0.315 [0.308, 0.323]
1.0 to 2.0	0.635 [0.595, 0.677]	0.273 [0.266, 0.281]
1.5 to 2.5	0.667 [0.628, 0.715]	0.241 [0.224, 0.259]
2.0 to 3.0	0.660 [0.600, 0.713]	0.221 [0.205, 0.238]
2.5 to 3.5	0.678 [0.614, 0.757]	0.197 [0.175, 0.214]
3.0 to 4.0	0.648 [0.574, 0.707]	0.197 [0.179, 0.221]
3.5 to 4.5	0.586 [0.525, 0.638]	0.202 [0.180, 0.229]
4.0 to 5.0	0.647 [0.590, 0.754]	0.192 [0.168, 0.217]
4.5 to 5.5	0.667 [0.582, 0.773]	0.184 [0.159, 0.220]
5.0 to 6.0	0.603 [0.496, 0.696]	0.170 [0.144, 0.207]
5.5 to 6.5	0.671 [0.576, 0.786]	0.173 [0.145, 0.202]
6.0 to 7.0	0.735 [0.663, 0.794]	0.196 [0.166, 0.219]
6.5 to 7.5	0.675 [0.565, 0.769]	0.202 [0.168, 0.231]
7.0 to 8.0	0.620 [0.518, 0.740]	0.187 [0.144, 0.217]
7.5 to 8.5	0.647 [0.538, 0.787]	0.183 [0.146, 0.222]

Table 13: **External validation of predictions of upgrading in Johns Hopkins Active Surveillance cohort.** The area under the receiver operating characteristic curve or AUC (measure of discrimination) and mean absolute prediction error or MAPE (measure of calibration) are calculated over the follow-up period at a gap of 6 months. In addition bootstrapped 95% confidence intervals (CI) are also presented.

Follow-up period (years)	AUC (95% CI)	MAPE (95%CI)
0.0 to 1.0	0.662 [0.586, 0.715]	0.254 [0.245, 0.265]
0.5 to 1.5	0.653 [0.603, 0.707]	0.229 [0.219, 0.240]
1.0 to 2.0	0.672 [0.604, 0.744]	0.128 [0.115, 0.141]
1.5 to 2.5	0.722 [0.652, 0.792]	0.095 [0.081, 0.111]
2.0 to 3.0	0.717 [0.638, 0.777]	0.112 [0.100, 0.123]
2.5 to 3.5	0.587 [0.493, 0.704]	0.144 [0.129, 0.154]
3.0 to 4.0	0.613 [0.486, 0.742]	0.141 [0.126, 0.156]
3.5 to 4.5	0.690 [0.594, 0.783]	0.115 [0.100, 0.133]
4.0 to 5.0	0.666 [0.572, 0.754]	0.121 [0.104, 0.147]
4.5 to 5.5	0.688 [0.519, 0.779]	0.137 [0.119, 0.161]
5.0 to 6.0	0.735 [0.676, 0.820]	0.126 [0.102, 0.152]
5.5 to 6.5	0.674 [0.581, 0.765]	0.143 [0.121, 0.172]
6.0 to 7.0	0.597 [0.472, 0.712]	0.163 [0.126, 0.195]

Table 14: **External validation of predictions of upgrading in Memorial Sloan Kettering Cancer Center Active Surveillance cohort.** The area under the receiver operating characteristic curve or AUC (measure of discrimination) and mean absolute prediction error or MAPE (measure of calibration) are calculated over the follow-up period at a gap of 6 months. In addition bootstrapped 95% confidence intervals (CI) are also presented.

Follow-up period (years)	AUC (95% CI)	MAPE (95%CI)
0.0 to 1.0	0.628 [0.577, 0.688]	0.317 [0.316, 0.318]
0.5 to 1.5	0.606 [0.532, 0.657]	0.301 [0.290, 0.311]
1.0 to 2.0	0.599 [0.518, 0.671]	0.230 [0.207, 0.256]
1.5 to 2.5	0.581 [0.504, 0.663]	0.198 [0.168, 0.235]
2.0 to 3.0	0.671 [0.599, 0.741]	0.208 [0.182, 0.232]
2.5 to 3.5	0.703 [0.610, 0.777]	0.218 [0.197, 0.246]
3.0 to 4.0	0.629 [0.499, 0.706]	0.226 [0.194, 0.259]
3.5 to 4.5	0.664 [0.589, 0.756]	0.225 [0.199, 0.262]
4.0 to 5.0	0.747 [0.642, 0.841]	0.215 [0.188, 0.247]
4.5 to 5.5	0.719 [0.597, 0.852]	0.194 [0.165, 0.232]
5.0 to 6.0	0.698 [0.565, 0.792]	0.174 [0.136, 0.227]

Table 15: **External validation of predictions of upgrading in King's College London Active Surveillance cohort.** The area under the receiver operating characteristic curve or AUC (measure of discrimination) and mean absolute prediction error or MAPE (measure of calibration) are calculated over the follow-up period at a gap of 6 months. In addition bootstrapped 95% confidence intervals (CI) are also presented.

Follow-up period (years)	AUC (95% CI)	MAPE (95%CI)
0.0 to 1.0	0.589 [0.514, 0.653]	0.430 [0.407, 0.450]
0.5 to 1.5	0.660 [0.550, 0.742]	0.453 [0.431, 0.474]
1.0 to 2.0	0.683 [0.604, 0.753]	0.416 [0.396, 0.445]
1.5 to 2.5	0.691 [0.621, 0.766]	0.271 [0.246, 0.297]
2.0 to 3.0	0.689 [0.616, 0.785]	0.319 [0.282, 0.344]

Table 16: **External validation of predictions of upgrading in Michigan Urological Surgery Improvement Collaborative Active Surveillance cohort.** The area under the receiver operating characteristic curve or AUC (measure of discrimination) and mean absolute prediction error or MAPE (measure of calibration) are calculated over the follow-up period at a gap of 6 months. In addition bootstrapped 95% confidence intervals (CI) are also presented.

Follow-up period (years)	AUC (95% CI)	MAPE (95%CI)
0.0 to 1.0	0.639 [0.607, 0.672]	0.461 [0.450, 0.469]
0.5 to 1.5	0.617 [0.588, 0.652]	0.446 [0.441, 0.453]
1.0 to 2.0	0.599 [0.553, 0.632]	0.331 [0.317, 0.348]

161 Appendix C. Personalized Biopsies Based on Cause-Specific Cu- 162 mulative Upgrading-Risk

163 Consider some real patients from the PRIAS database shown in Figure 9–
164 11. In line with the protocols of most AS cohorts [12], we first schedule a
165 compulsory biopsy at year one of follow-up. This promises early detection
166 of Gleason upgrade for patients misdiagnosed as low-grade cancer patients,
167 or patients who chose AS despite having a higher grade at diagnosis. We
168 also maintain a recommended minimum gap of one year between consecu-
169 tive biopsies [11]. That is, we intend to develop personalized schedule of
170 biopsies for these patients starting from the second year. The added benefit
171 of planning biopsies year two onwards is that due to the longitudinal mea-
172 surements accumulated over two years, and year one biopsy results, we are
173 able to make reasonably accurate predictions of the cause-specific cumulative
174 upgrading-risk.

Using the joint model fitted to the PRIAS dataset, we first obtain a pa-
tient’s cause-specific cumulative upgrading-risk over the entire future follow-
up period (see 4), given their accumulated two year clinical data. Typically
biopsies may be decided on the same visit on which PSA is measured. Let
 $U = u_1, \dots, u_L$ represent a schedule of such visits (e.g., every six months in
prostate cancer for PSA measurement), where $u_1 = v$ is also the time of the
current visit, and u_L is the horizon up to which we intend to plan biopsies.
Depending upon how much training/validation data is available, this horizon
differs between cohorts (Table 17). First, we make L successive decisions for
conducting biopsies on each of the L future visit times $u_l \in U$. Specifically,
we decide to conduct a biopsy at time u_l if the conditional cumulative-risk
of progression at u_l is larger than a certain risk threshold $0 \leq \kappa \leq 1$ (e.g.,
 $\kappa = 10\%$ risk). If a biopsy gets planned at time u_l , then the successive biopsy
decision at time u_{l+1} is made using an updated cumulative-risk profile. This
updated cumulative-risk profile accounts for the possibility that progression
may occur after time $u_l < T_j^*$. The biopsy decisions on each future visit time
 u_l are defined as:

$$Q_j^\kappa(u_l | t_l, v) = I\{R_j(u_l | t_l, v) \geq \kappa\},$$

$$t_l = \begin{cases} t, & \text{if } l = 1 \\ t_{l-1}, & \text{if } Q_j^\kappa(u_{l-1} | t_{l-1}, v) = 0, l \geq 2 \\ u_{l-1}, & \text{if } Q_j^\kappa(u_{l-1} | t_{l-1}, v) = 1, l \geq 2 \end{cases}.$$

The cumulative-risk $R_j(u_l | t_l, v)$ at future visit time u_l utilizes the time t_l

as the time of the last conducted biopsy on which progression may not be observed. However, the contribution of the observed longitudinal data $\mathcal{Y}_j(v)$ in the risk function remains the same over all time points in U . The biopsy decision at time u_l is denoted by $Q_j^\kappa(u_l | t_l, v)$. Via the indicator function $I(\cdot)$ it obtains a value 1 (or 0) when a biopsy is to be conducted (or not conducted) at time u_l . The subset of future time points in U on which a biopsy is to be performed results into a personalized schedule of planned future biopsies, given by:

$$S_j^\kappa(U | t, v) = \{u_l \in U | Q_j^\kappa(u_l | t_l, v) = 1\}. \quad (6)$$

175 The personalized schedule in (6) is updated as more patient data becomes
176 available over subsequent follow-up visits.

177 *Appendix C.1. Expected Time Delay in Detecting Progression*

178 The schedule $S_j^\kappa(U | t, v)$ manifests a personalized biopsy plan for the
179 j -the patient. However, the the time delay in detecting progression that
180 may subsequently be observed, depends on the true time of progression T_j^*
181 of the patient. Since two different patients with the same timing of biopsies
182 will expect different time delays, we estimate it in a patient-specific manner
183 as well. Although, this calculation is not limited to personalized schedules
184 only, but can be done for any schedule S of biopsies with N time points
185 $S = \{s_n | n = 1, \dots, N\}$.

For each of the N planned biopsies there exist N possible time intervals $s_{n-1} < T_j^* \leq s_n$ in which progression may be observed. Correspondingly, there are N possible time delays in detecting progression $s_n - T_j^*$. Given a schedule S , the true time delay in detecting progression D_j that the patient will experience can be defined as:

$$D_j(S | t) = \left\{ \begin{array}{ll} s_1 - T_j^*, & \text{if } t < T_j^* \leq s_1 \\ \dots & \\ s_N - T_j^*, & \text{if } s_{N-1} < T_j^* \leq s_N \end{array} \right\}. \quad (7)$$

The time delay is cannot be defined for the scenario in which the patient obtains progression after the time of the last biopsy in the schedule $T_j^* > s_N$. Hence, this delay should be interpreted as the delay that will be observed if the patient will experience upgrading before time of the last planned biopsy at $T_j^* \leq s_N$. To estimate the expected value of $D_j(\cdot)$ in a patient-specific manner, we exploit the personalized cumulative-risk profile of the patient

defined in (4). Specifically, the expected time delay $E\{D_j(\cdot)\}$ can be calculated as the weighted sum of N possible time delays defined in (7). The n -th weight is equal to the probability of the patient obtaining progression in the n -th interval $s_{n-1} < T_j^* \leq s_n$.

$$\begin{aligned}
 E\{D_j(S | t)\} &= \sum_{n=1}^N \left\{ s_n - E(T_j^* | s_{n-1}, s_n, v) \right\} \\
 &\quad \times \Pr\left\{ s_{n-1} < T_j^* \leq s_n \mid T_j^* \leq s_N, (Y)_j(v), \mathcal{A}_n \right\}, \quad s_0 = t \\
 E(T_j^* | s_{n-1}, s_n, v) &= s_{n-1} + \int_{s_{n-1}}^{s_n} \Pr\left\{ T_j^* \geq u \mid s_{n-1} < T_j^* \leq s_n, \mathcal{Y}_j(v), \mathcal{A}_n \right\} du,
 \end{aligned}$$

186 where $E(T_j^* | s_{n-1}, s_n, v)$ denotes the conditional expected time of progression
 187 for the scenario $s_{n-1} < T_j^* \leq s_n$, and is calculated as the area under the
 188 corresponding survival curve.

189 The personalized expected time delay in detecting progression has the
 190 advantage that it is updated over follow-up as more patient data becomes
 191 available. Since it can be calculated for any schedule, patients and doctors
 192 can utilize it along with the plan of biopsies to compare schedules before
 193 making a decision. Although, in order to have a fair comparison of time
 194 delays between different schedules for the same patient, a compulsory biopsy
 195 at a common horizon time point should be planned in all schedules.

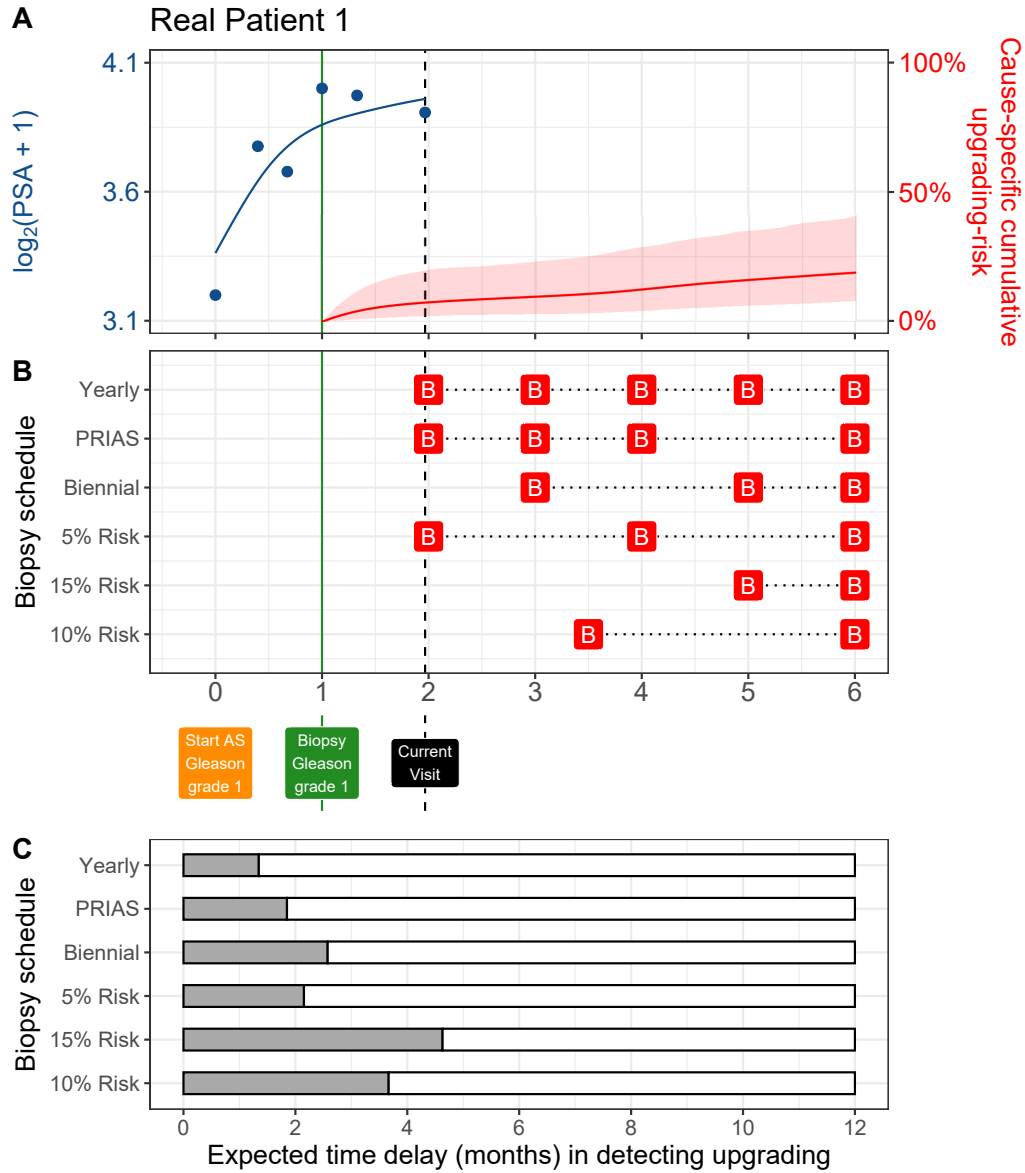


Figure 9: **Personalized and fixed schedules of biopsies for patient 1.** **Panel A:** shows the observed and fitted $\log_2(\text{PSA} + 1)$ measurements (Equation 1), and the dynamic cause-specific cumulative upgrading-risk (see Appendix B) over follow-up period. **Panel B** shows the personalized and fixed schedules of biopsies with a 'B' indicating times of biopsies. **Panel C** compares various schedules in terms of the expected delay in detection of upgrading if they are followed. A compulsory biopsy was scheduled at year six (maximum biopsy scheduling time in PRIAS, Supplementary C) in all schedules for a meaningful comparison between them.

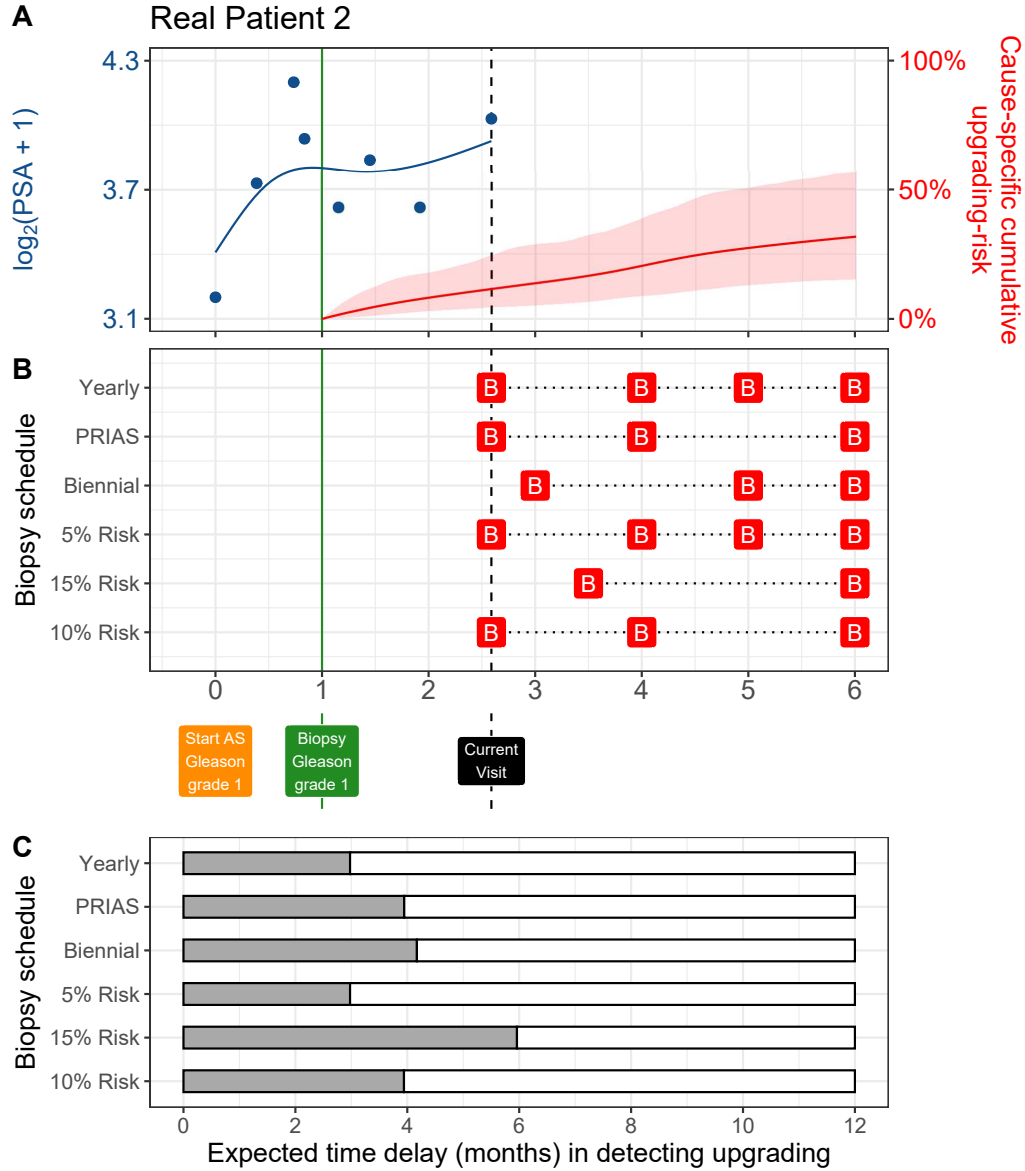


Figure 10: **Personalized and fixed schedules of biopsies for patient 2.** **Panel A:** shows the observed and fitted $\log_2(\text{PSA} + 1)$ measurements (Equation 1), and the dynamic cause-specific cumulative upgrading-risk (see Appendix B) over follow-up period. **Panel B** shows the personalized and fixed schedules of biopsies with a 'B' indicating times of biopsies. **Panel C** compares various schedules in terms of the expected delay in detection of upgrading if they are followed. A compulsory biopsy was scheduled at year six (maximum biopsy scheduling time in PRIAS, Supplementary C) in all schedules for a meaningful comparison between them.

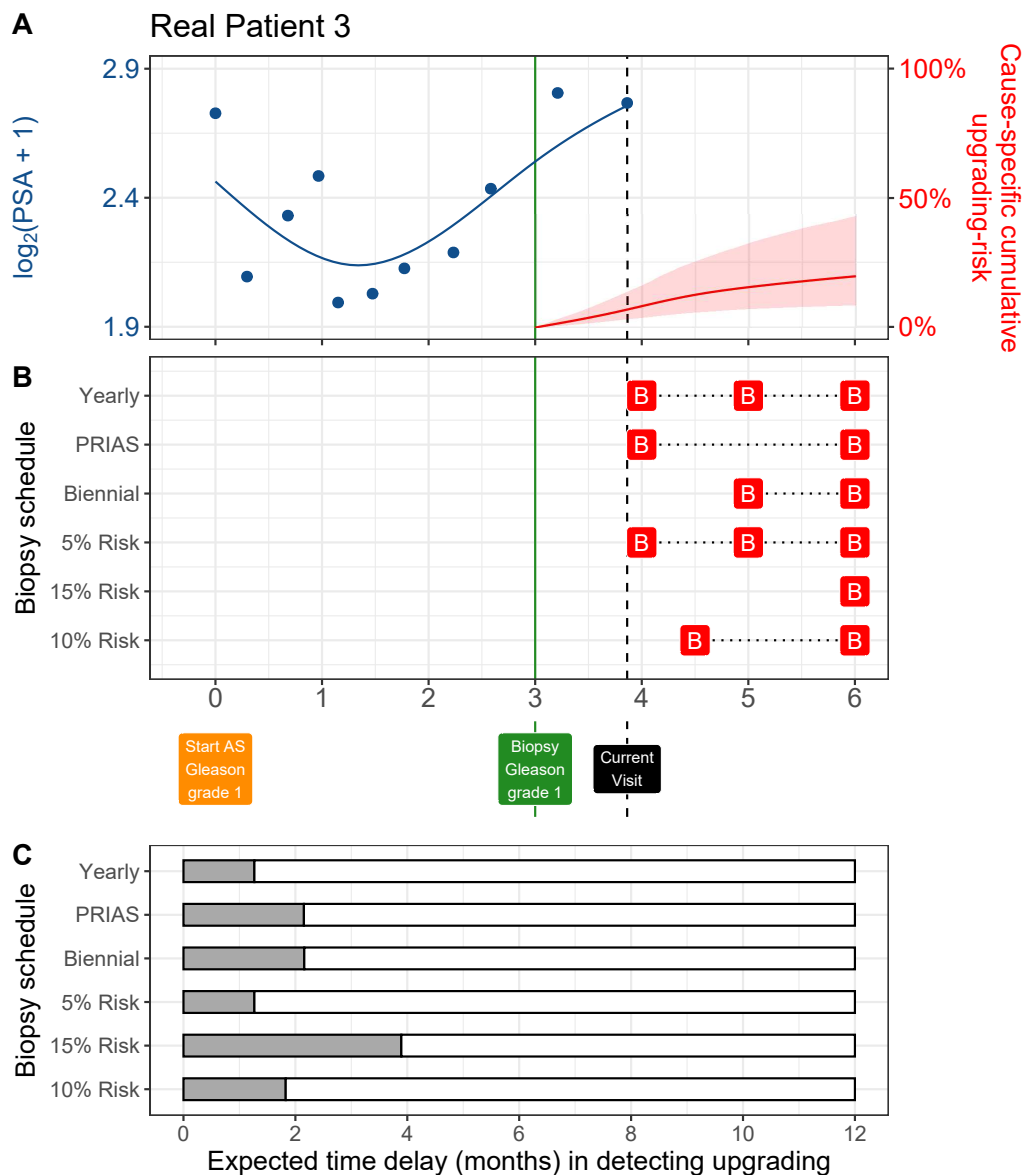


Figure 11: **Personalized and fixed schedules of biopsies for patient 3.** **Panel A:** shows the observed and fitted $\log_2(\text{PSA} + 1)$ measurements (Equation 1), and the dynamic cause-specific cumulative upgrading-risk (see Appendix B) over follow-up period. **Panel B** shows the personalized and fixed schedules of biopsies with a 'B' indicating times of biopsies. **Panel C** compares various schedules in terms of the expected delay in detection of upgrading if they are followed. A compulsory biopsy was scheduled at year six (maximum biopsy scheduling time in PRIAS, Supplementary C) in all schedules for a meaningful comparison between them.

Table 17: **Maximum follow-up period up to which we can reliably make personalized schedules.** In each cohort, this time point is chosen such that there are at least 10 patients who experience upgrading after this time point. Full names of Cohorts are *PRIAS*: Prostate Cancer International Active Surveillance, *Toronto*: University of Toronto Active Surveillance, *Hopkins*: Johns Hopkins Active Surveillance, *MSKCC*: Memorial Sloan Kettering Cancer Center Active Surveillance, *KCL*: King's College London Active Surveillance, *MUSIC*: Michigan Urological Surgery Improvement Collaborative Active Surveillance, *UCSF*: University of California San Francisco Active Surveillance.

Cohort	Maximum Personalized Schedule Time (years)
PRIAS	6
KCL	3
MUSIC	2
Toronto	8
MSKCC	6
Hopkins	7
UCSF	8.5

Appendix D. Web Application for Practical Use of Personalized Schedule of Biopsies

We implemented our methodology in a web-application to assist patients and doctors in better decision making. It works on desktop as well as mobile devices. The cohorts that are currently supported in this web-application are PRIAS and the largest six cohorts from the GAP3 database [6]. These are the University of Toronto AS (Toronto), Johns Hopkins AS (Hopkins), Memorial Sloan Kettering Cancer Center AS (MSKCC), King's College London AS (KCL), Michigan Urological Surgery Improvement Collaborative AS (MUSIC), and University of California San Francisco Active Surveillance (UCSF). The web-application is hosted at https://emcbiostatistics.shinyapps.io/prias_biopsy_recommender/.

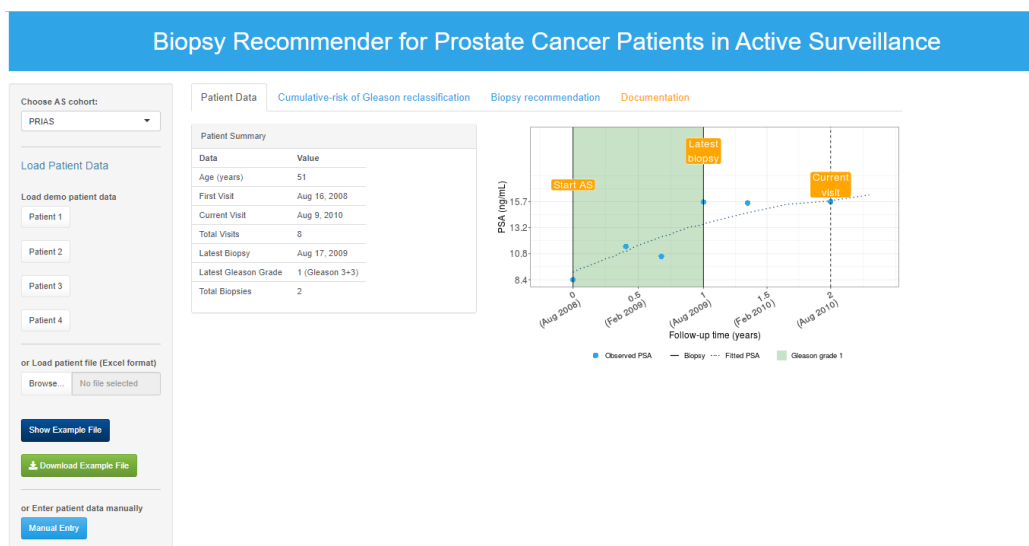


Figure 12: Landing page of the web-application. Panel on the left allows users to load patient data and panel on the right provides information. Patient data can be entered manually, or via Excel files. In addition, demo patient data is already uploaded to assist users in understanding the web-application.

208 Appendix E. Source Code

209 The R code for fitting the joint model to the PRIAS dataset, is at [https:](https://github.com/anirudhtomer/prias/tree/master/src/clinical_gap3)
 210 [//github.com/anirudhtomer/prias/tree/master/src/clinical_gap3](https://github.com/anirudhtomer/prias/tree/master/src/clinical_gap3). We
 211 refer to this location as ‘R_HOME’ in the rest of this document.

212 *Appendix E.1. Fitting the Joint Model to the PRIAS dataset*

213 **Accessing the dataset:** The PRIAS dataset is not openly accessible.
 214 However, access to the database can be requested via the contact links at
 215 <https://www.prias-project.org>.

216
 217 **Formatting the dataset:** This dataset however is in the so-called wide
 218 format and also requires removal of incorrect entries. This can be done
 219 via the R script `R_HOME/dataset_cleaning.R`. This will lead to two R
 220 objects, namely ‘`prias_final.id`’ and ‘`prias_long_final`’. The ‘`prias_final.id`’ ob-
 221 ject contains information about time of upgrading for PRIAS patients. The
 222 ‘`prias_long_final`’ object contains longitudinal PSA measurements, the time
 223 of biopsies and results of biopsies.

224
 225 **Fitting the joint model:** We use a joint model for time to event and
 226 longitudinal data to model the evolution of PSA measurements over time,
 227 and to simultaneously model their association with the risk of upgrading.
 228 The R package we use for this purpose is called **JMbayes** ([https://cran.r-](https://cran.r-project.org/web/packages/JMbayes/JMbayes.pdf)
 229 [project.org/web/packages/JMbayes/JMbayes.pdf](https://cran.r-project.org/web/packages/JMbayes/JMbayes.pdf)). The API we use, how-
 230 ever, are currently not hosted on CRAN, and can be found here: [https:](https://github.com/anirudhtomer/JMbayes)
 231 [//github.com/anirudhtomer/JMbayes](https://github.com/anirudhtomer/JMbayes). The joint model can be fitted via
 232 the script `R_HOME/analysis.R`. It takes roughly 6 hours to run on an Intel
 233 core-i5 machine with 4 cores, and 8GB of RAM.

234 The graphs presented in the main manuscript, and the supplementary
 235 material can be generated by the scripts in `R_HOME/plots/`.

236 *Appendix E.2. Validation of Predictions of Upgrading*

237 Validations can be done using the scripts `R_HOME/validation/auc_brier/`
 238 `auc_calculator.R`, and `R_HOME/validation/auc_brier/gof_calculator.`
 239 `R`. For external validation access to GAP3 database is required.

240 *Appendix E.3. Creating Personalized Schedules of Biopsies*

241 Once a joint model is fitted to the PRIAS dataset, personalized schedules
242 of biopsies based on risk of upgrading for new patients can be developed us-
243 ing the script `R_HOME/scheduleCreator.R`. This script also provides fixed
244 biopsy schedules for the patients. In addition with each schedule, the ex-
245 pected delay in detection of upgrading is also provided.

246 *Appendix E.4. Source Code for Web Application*

247 Source for the shiny web application which provides biopsy schedules for
248 patients can be found at `R_HOME/shinyapp`

249 **Appendix F. Appendix A. Members of The Movember Founda-**
 250 **tions Global Action Plan Prostate Cancer Active Surveil-**
 251 **lance (GAP3) consortium**

252 *Principle Investigators:* Bruce Trock (Johns Hopkins University, The
 253 James Buchanan Brady Urological Institute, Baltimore, USA), Behfar Ehdaie
 254 (Memorial Sloan Kettering Cancer Center, New York, USA), Peter Car-
 255 roll (University of California San Francisco, San Francisco, USA), Christo-
 256 pher Filson (Emory University School of Medicine, Winship Cancer Insti-
 257 tute, Atlanta, USA), Jeri Kim / Christopher Logothetis (MD Anderson
 258 Cancer Centre, Houston, USA), Todd Morgan (University of Michigan and
 259 Michigan Urological Surgery Improvement Collaborative (MUSIC), Michi-
 260 gan, USA), Laurence Klotz (University of Toronto, Sunnybrook Health Sci-
 261 ences Centre, Toronto, Ontario, Canada), Tom Pickles (University of British
 262 Columbia, BC Cancer Agency, Vancouver, Canada), Eric Hyndman (Uni-
 263 versity of Calgary, Southern Alberta Institute of Urology, Calgary, Canada),
 264 Caroline Moore (University College London & University College London
 265 Hospital Trust, London, UK), Vincent Gnanapragasam (University of Cam-
 266 bridge & Cambridge University Hospitals NHS Foundation Trust, Cam-
 267 bridge, UK), Mieke Van Hemelrijck (King's College London, London, UK
 268 & Guys and St Thomas NHS Foundation Trust, London, UK), Prokar Das-
 269 gupta (Guys and St Thomas NHS Foundation Trust, London, UK), Chris
 270 Bangma (Erasmus Medical Center, Rotterdam, The Netherlands/ represen-
 271 tative of Prostate cancer Research International Active Surveillance (PRIAS)
 272 consortium), Monique Roobol (Erasmus Medical Center, Rotterdam, The
 273 Netherlands/ representative of Prostate cancer Research International Active
 274 Surveillance (PRIAS) consortium), Arnauld Villers (Lille University Hospi-
 275 tal Center, Lille, France), Antti Rannikko (Helsinki University and Helsinki
 276 University Hospital, Helsinki, Finland), Riccardo Valdagni (Department of
 277 Oncology and Hemato-oncology, Universit degli Studi di Milano, Radia-
 278 tion Oncology 1 and Prostate Cancer Program, Fondazione IRCCS Istituto
 279 Nazionale dei Tumori, Milan, Italy), Antoinette Perry (University College
 280 Dublin, Dublin, Ireland), Jonas Hugosson (Sahlgrenska University Hospital,
 281 Gteborg, Sweden), Jose Rubio-Briones (Instituto Valenciano de Oncologa,
 282 Valencia, Spain), Anders Bjartell (Skne University Hospital, Malm, Swe-
 283 den), Lukas Hefermehl (Kantonsspital Baden, Baden, Switzerland), Lee Lui
 284 Shiong (Singapore General Hospital, Singapore, Singapore), Mark Fryden-
 285 berg (Monash Health; Monash University, Melbourne, Australia), Yoshiyuki

286 Kakehi / Mikio Sugimoto (Kagawa University Faculty of Medicine, Kagawa,
 287 Japan), Byung Ha Chung (Gangnam Severance Hospital, Yonsei University
 288 Health System, Seoul, Republic of Korea)

289 *Pathologist:* Theo van der Kwast (Princess Margaret Cancer Centre,
 290 Toronto, Canada). Technology Research Partners: Henk Obbink (Royal
 291 Philips, Eindhoven, the Netherlands), Wim van der Linden (Royal Philips,
 292 Eindhoven, the Netherlands), Tim Hulsen (Royal Philips, Eindhoven, the
 293 Netherlands), Cees de Jonge (Royal Philips, Eindhoven, the Netherlands).

294 *Advisory Regional statisticians:* Mike Kattan (Cleveland Clinic, Cleve-
 295 land, Ohio, USA), Ji Xinge (Cleveland Clinic, Cleveland, Ohio, USA), Ken-
 296 neth Muir (University of Manchester, Manchester, UK), Artitaya Lophatananon
 297 (University of Manchester, Manchester, UK), Michael Fahey (Epworth Health-
 298 Care, Melbourne, Australia), Ewout Steyerberg (Erasmus Medical Center,
 299 Rotterdam, The Netherlands), Daan Nieboer (Erasmus Medical Center, Rot-
 300 terdam, The Netherlands); Liying Zhang (University of Toronto, Sunnybrook
 301 Health Sciences Centre, Toronto, Ontario, Canada)

302 *Executive Regional statisticians:* Ewout Steyerberg (Erasmus Medical
 303 Center, Rotterdam, The Netherlands), Daan Nieboer (Erasmus Medical Cen-
 304 ter, Rotterdam, The Netherlands); Kerri Beckmann (King's College London,
 305 London, UK & Guys and St Thomas NHS Foundation Trust, London, UK),
 306 Brian Denton (University of Michigan, Michigan, USA), Andrew Hayen (Uni-
 307 versity of Technology Sydney, Australia), Paul Boutros (Ontario Institute of
 308 Cancer Research, Toronto, Ontario, Canada).

309 *Clinical Research Partners IT Experts:* Wei Guo (Johns Hopkins Uni-
 310 versity, The James Buchanan Brady Urological Institute, Baltimore, USA),
 311 Nicole Benfante (Memorial Sloan Kettering Cancer Center, New York, USA),
 312 Janet Cowan (University of California San Francisco, San Francisco, USA),
 313 Dattatraya Patil (Emory University School of Medicine, Winship Cancer In-
 314 stitute, Atlanta, USA), Emily Tolosa (MD Anderson Cancer Centre, Hous-
 315 ton, Texas, USA), Tae-Kyung Kim (University of Michigan and Michigan
 316 Urological Surgery Improvement Collaborative, Ann Arbor, Michigan, USA),
 317 Alexandre Mamedov (University of Toronto, Sunnybrook Health Sciences
 318 Centre, Toronto, Ontario, Canada), Vincent LaPointe (University of British
 319 Columbia, BC Cancer Agency, Vancouver, Canada), Trafford Crump (Uni-
 320 versity of Calgary, Southern Alberta Institute of Urology, Calgary, Canada),
 321 Vasilis Stavrinides (University College London & University College Lon-
 322 don Hospital Trust, London, UK), Jenna Kimberly-Duffell (University of
 323 Cambridge & Cambridge University Hospitals NHS Foundation Trust, Cam-

bridge, UK), Aida Santaolalla (King's College London, London, UK & Guys
and St Thomas NHS Foundation Trust, London, UK), Daan Nieboer (Eras-
mus Medical Center, Rotterdam, The Netherlands), Jonathan Olivier (Lille
University Hospital Center, Lille, France), Tiziana Rancati (Fondazione IR-
CCS Istituto Nazionale dei Tumori di Milano, Milan, Italy), Heln Ahlgren
(Sahlgrenska University Hospital, Gteborg, Sweden), Juanma Mascars (Insti-
tuto Valenciano de Oncologa, Valencia, Spain), Annica Lfgren (Skne Univer-
sity Hospital, Malm, Sweden), Kurt Lehmann (Kantonsspital Baden, Baden,
Switzerland), Catherine Han Lin (Monash University and Epworth Health-
Care, Melbourne, Australia), Hiromi Hiram (Kagawa University, Kagawa,
Japan), Kwang Suk Lee (Yonsei University College of Medicine, Gangnam
Severance Hospital, Seoul, Korea).

Research Advisory Committee: Guido Jenster (Erasmus MC, Rotterdam,
the Netherlands), Anssi Auvinen (University of Tampere, Tampere, Finland),
Anders Bjartell (Skne University Hospital, Malm, Sweden), Masoom Haider
(University of Toronto, Toronto, Canada), Kees van Bochove (The Hyve
B.V. Utrecht, Utrecht, the Netherlands), Ballentine Carter (Johns Hopkins
University, Baltimore, USA until 2018).

Management team: Sam Gledhill (Movember Foundation, Melbourne,
Australia), Mark Buzza / Michelle Kouspou (Movember Foundation, Mel-
bourne, Australia), Chris Bangma (Erasmus Medical Center, Rotterdam,
The Netherlands), Monique Roobol (Erasmus Medical Center, Rotterdam,
The Netherlands), Sophie Bruinsma / Jozien Helleman (Erasmus Medical
Center, Rotterdam, The Netherlands).

References

1. Epstein JI, Egevad L, Amin MB, Delahunt B, Srigley JR, Humphrey PA.
The 2014 international society of urological pathology (isup) consensus
conference on gleason grading of prostatic carcinoma. *The American
journal of surgical pathology* 2016;40(2):244–52.
2. Pearson JD, Morrell CH, Landis PK, Carter HB, Brant LJ. Mixed-
effects regression models for studying the natural history of prostate
disease. *Statistics in Medicine* 1994;13(5-7):587–601.
3. Lin H, McCulloch CE, Turnbull BW, Slate EH, Clark LC. A latent
class mixed model for analysing biomarker trajectories with irregularly
scheduled observations. *Statistics in Medicine* 2000;19(10):1303–18.

- 359 4. De Boor C. A practical guide to splines; vol. 27. Springer-Verlag New
360 York; 1978.
- 361 5. Eilers PH, Marx BD. Flexible smoothing with B-splines and penalties.
362 *Statistical Science* 1996;11(2):89–121.
- 363 6. Bruinsma SM, Zhang L, Roobol MJ, Bangma CH, Steyerberg EW,
364 Nieboer D, Van Hemelrijck M, consortium MFGAPPCASG, Trock B,
365 Ehdaie B, et al. The movember foundation’s gap3 cohort: a profile of
366 the largest global prostate cancer active surveillance database to date.
367 *BJU international* 2018;121(5):737–44.
- 368 7. Turnbull BW. The empirical distribution function with arbitrarily
369 grouped, censored and truncated data. *Journal of the Royal Statisti-*
370 *cal Society Series B (Methodological)* 1976;38(3):290–5.
- 371 8. Rizopoulos D. The R package JMbayes for fitting joint models for lon-
372 gitudinal and time-to-event data using MCMC. *Journal of Statistical*
373 *Software* 2016;72(7):1–46.
- 374 9. Rizopoulos D, Molenberghs G, Lesaffre EM. Dynamic predictions with
375 time-dependent covariates in survival analysis using joint modeling and
376 landmarking. *Biometrical Journal* 2017;59(6):1261–76.
- 377 10. Steyerberg EW, Vickers AJ, Cook NR, Gerds T, Gonen M, Obuchowski
378 N, Pencina MJ, Kattan MW. Assessing the performance of prediction
379 models: a framework for some traditional and novel measures. *Epidemi-*
380 *ology (Cambridge, Mass)* 2010;21(1):128.
- 381 11. Bokhorst LP, Alberts AR, Rannikko A, Valdagni R, Pickles T, Kakehi Y,
382 Bangma CH, Roobol MJ, PRIAS study group . Compliance rates with
383 the Prostate Cancer Research International Active Surveillance (PRIAS)
384 protocol and disease reclassification in noncompliers. *European Urology*
385 2015;68(5):814–21.
- 386 12. Nieboer D, Tomer A, Rizopoulos D, Roobol MJ, Steyerberg EW. Active
387 surveillance: a review of risk-based, dynamic monitoring. *Translational*
388 *andrology and urology* 2018;7(1):106–15.